The 1st international symposium on VLEO missions and technologies
June 28-29, 2021 Manchester, UK

Accelerated AO-induced polyimide erosion in VLEO by simultaneous collisions of hyperthermal N_2 molecules: ground-based experiments

Sasuga Horimoto, Atsushi Fujita,
Wataru Ide, Kumiko Yokota, Masahito Tagawa

Department of Mechanical Engineering, Kobe University, Rikko-dai 1-1, Nada, Kobe 657-8501 Japan

Corresponding authors: Sasuga Horimoto (215t362t@stu.kobe-u.ac.jp)
Masahito Tagawa (tagawa@mech.kobe-u.ac.jp)

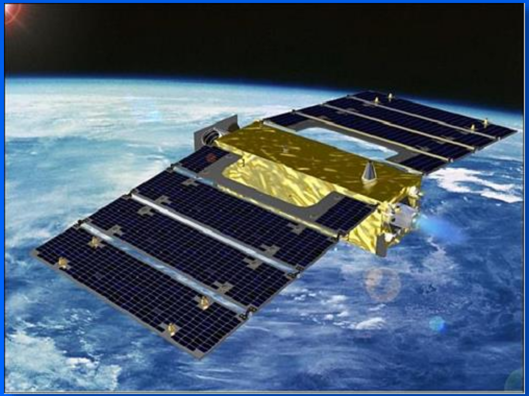

1. Introduction

It has been widely recognized that many carbon-based spacecraft materials are eroded by atomic oxygen (AO) in upper atmosphere of Earth. Because density of upper atmosphere of Earth decreases with altitude, AO-related problems are not concerned in geo synchronous orbit. In contrast, AO-related erosion becomes very serious concern for satellites which is orbiting low altitude.

In very low Earth orbit (VLEO) environment, where the altitude lower than 300 km, materials on the exterior surface of spacecraft encounter simultaneous collisions of not only AO but also N_2 due to composition variation of the atmosphere compared to conventional LEO at 400- 500 km in altitude. It has been reported by Minton that the hyperthermal collision of Ar at oxidized polyimide promotes desorption of CO and CO_2 from the oxidized polymer surfaces [1]. This experimental findings suggest the simultaneous collisions of AO and N_2 in VLEO environment may produce accelerated erosion of polyimide. Tagawa has also confirmed that the rate of mass loss of polyimide film was enhanced by simultaneous Ar bombardment during hyperthermal AO exposure [2]. These phenomena was confirmed in the ground-based simulations. However, the same increase in erosion rate of polyimide was recently confirmed by Yokota in the world's first material exposure experiment in VLEO aboard the superlow altitude test satellite (SLATS) launched December 23, 2017 [2]. She found that mass loss of polyimide coated on a QCM is not proportional to the AO density predicted by NRLMSISE-00 atmospheric model at the altitude of 216 km. She pointed out that this phenomenon could be explained by the variation in erosion yield, Ey, (average volume of material lost by single AO collision in the unit of cm3/atom) of polyimide in VLEO environment, namely, the Ey of polyimide by AO was increased linearly with N_2 fraction in the upper atmosphere of Earth. Thus, the acceleration effect of AO-induced polyimide erosion by chemically inert hyperthermal molecules such as N_2 or Ar is now confirmed both in laboratory and in orbit. This experimental results suggested that the material life in VLEO is considerably shorter than that predicted by the established erosion rate of 3.0E-24 cm3/atom in the ASTM standard [3]. However, this phenomenon has not yet understood in detail.

In this paper, a series of ground-based experiments on polyimide erosion in different collision energies of Ar is reported. Hyperthermal AO and Ar beam exposures were performed by the laser detonation beam source with dual pulsed sonic valve (dual-PSV) system especially developed for VLEO neutral gas simulations. The new data observed in this study is valuable to understand the erosion mechanism of materials in VLEO environment.

2. Experimental details

The laser detonation beam source, which has been used for studying material erosion in VLEO, was applied to form hyperthermal AO and Ar beams. Figure 1 shows the schematic drawing of the configuration of the facility [4]. The major components of this system are dual-PSV, CO_2 laser and time-of-flight (TOF) measuring system with quadrupole mass spectrometer (QMS). The dual-PSV equips two piezoelectric-driven actuators with elongation enlargement system. O_2 and Ar were ejected individually at different timing into a conical nozzle through two channel of dual-PSV system shown in Figure 2 (individual exposure mode) [5]. Effect of N_2 collision in VLEO was simulated by Ar collision in this ground-based simulations to prevent the decomposition of N_2 in the laser-induced plasma. Namely, the chemical nature of N_2 and CO_2 collision is ignored in this study. However, chemical reaction of N_2 and CO_2 is rather weak compared with that activated by AO, thus we believe the physical effect of N_2 collision is much more influences to the polymer degradation.

A TEA CO_2 laser with 5 -7 J/pulse is used to decompose O_2 molecules to AO and accelerate the molecules. The maximum repetition rate of the laser is 5 Hz which limits the overall performance of the system. TOF spectrum was used for characterizing the beam. The TOF measurement system was consisted of a QMS with an electron impact ionizer and a scintillation detector. The average beam energies of AO, O_2 and Ar components in the beam were analyzed using TOF spectra. The experiment was performed with a laser repetition rate of 4 Hz.

The sample used in this study was a polyimide-coated QCM. The polyimide film coated on a QCM sensor crystal is U-varnish A (Ube Industries, Ltd.)

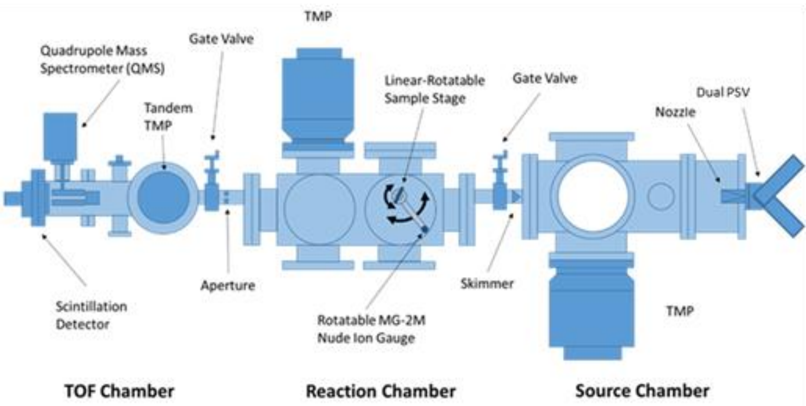

Firure 1 Configuration of the laser detonation atomic oxygen source.

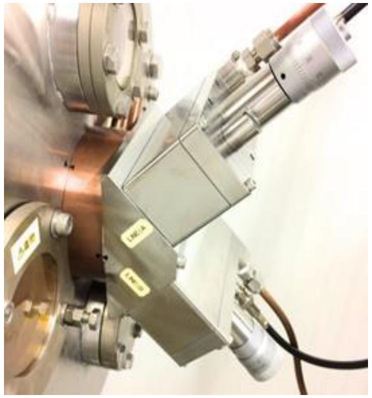

Figure 2 Dual PSV system which two piezoelectric-driven pulsed supersonic valves attached to the nozzle system of laser-detonation source.

3. Results and Discussion

3.1 Ar flux measurement

Flux measurement of AO is possible by using mass-loss of polyimide because the Ey has been established by the early shuttle flight as described in the previous section. This method is not applicable for Ar flux measurement. Most common method is to measure Ar beam flux is the ionization technique such as ionization vacuum gauges. However, ionization cross-section of Ar atom in the particular measurement system is unknown, a reference is needed for the absolute flux measurement of Ar.

In this study, we use flux-weighted TOF spectra of AO and AO flux measured by the PI-QCM were used as a reference of Ar flux measurement. Figure 3 shows the typical flux-weighted TOF spectra of AO, O_2 and Ar measured by the QMS. Difference in ionization probability due to the difference in beam velocity distribution was corrected in Figure 3 by considering the existing time in the ionizer. The average translational energies and the integrated intensities of each beam component were calculated from these spectra.

Each area of flux-weighted TOF spectra is proportional to the number of arriving atoms, because the same system was used for all TOF measurement.

Therefore, relative flux of AO, O_2 and Ar component in the same beam pulses are calculated by using established relative ionization cross-section previously measured in the same system [4]. Because absolute AO flux was measured by the PI-QCM, absolute O_2 and Ar fluxes are also calculated. Table 1 summarizes the results of AO and Ar beams formed by pure O_2 and Ar target gas. When O_2 gas is used as the target gas, undecomposed O_2 component (36%) remains in the AO beam. Three Ar beams with different energies are created (4.1, 5.9 and 7.3 eV). Absolute O_2 and Ar fluxes were calculated based on the flux-weighted TOF spectra and relative ionization cross-sections as described above.

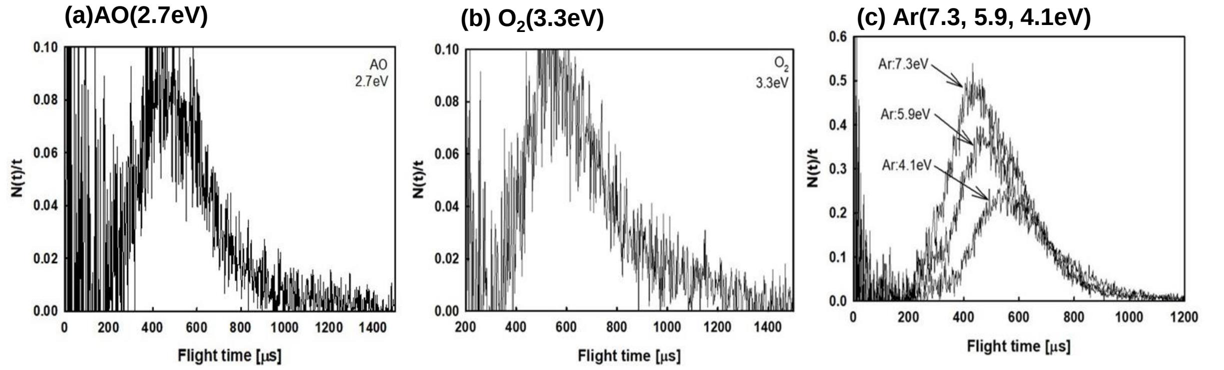
(a)AO(2.7eV) (b) O_2(3.3eV) (c) Ar(7.3, 5.9, 4.1eV)

Firure 3 The typical flux-weighted time-of-flight spectra.

Table 1 The results of AO and Ar beams formed by pure O_2 and Ar target gas.

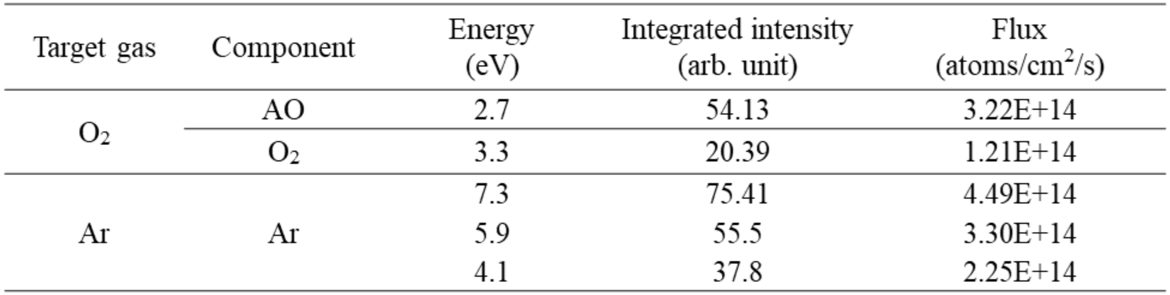

Target gas	Component	Energy (eV)	Integrated intensity (arb. unit)	Flux (atoms/cm^2/s)
O_2	AO	2.7	54.13	3.22E+14
	O_2	3.3	20.39	1.21E+14
Ar	Ar	7.3	75.41	4.49E+14
		5.9	55.5	3.30E+14
		4.1	37.8	2.25E+14

3.2 Mass-loss of PI-QCM under AO and Ar exposures

AO/O_2 and Ar beam pulses are formed by the each channel of dual-PSV system and number of pulses of both channels are controlled to adjust the flux ratio of AO and Ar beams. Because the repetition rate of the dual-PSV system is restricted by that of laser (5Hz), high Ar fraction beam conditions are created by decreasing the repetition rate of AO pulses while that of Ar pulses are kept constant. On the other hand, low Ar condition was created by reducing the repetition rate of Ar pulses.

The frequency shift of PI-QCM during the exposure of various Ar fraction beam (7.3 eV) is shown in Figure 4. It is clearly indicated that the frequency shift of PI-QCM gradually increases with increasing Ar fraction in the Ar faction lower than 60%, and then start decreasing to zero at Ar 100%. This non-linear phenomenon was explained the erosion mechanism considering two-stage erosion mechanism, i.e., oxidation and desorption stages [6]. In the two-stage model in the PI erosion by hyperthermal AO, H abstraction mechanism is considered to be the first step of a series of reactions resulting in mass loss. AO absorbs at the dangling bonds and forms oxide which leads to mass increase. Due to large electronegativity of O, C-C backbone is weakened, and C atoms originally included in the polymer structure is removed from the surface by forming volatile products such as CO and CO_2 which leads to mass-loss. This model was obvious in the initial stage of PI erosion by AO. By considering two stage reaction, the rate-limiting step of mass-loss of PI changes by the balance of rate of oxidation and desorption.

In the high Ar fraction conditions (>Ar 60%), the rate of desorption of oxidized products by collision-induced desorption (CID) process is faster than that of oxidation. Therefore, the rate-limiting step of mass-loss is the oxidation stage. As a result, no mass-loss should be observed at 100% Ar condition (no AO pulse is given). This is confirmed in Figure 5 which shows the result of 100% Ar beam exposure. In Figure 5, time history of resonant frequencies of PI-QCM under 100% Ar and 0%Ar (100% AO/O2) exposures are indicated. It is clear that collision of Ar at 6.2 eV without oxidation does not show the mass loss whereas exposures AO only leads to clear mass-loss of PI. This is because the AO itself has collision energy to be used in desorption process. This explains the phenomenon that frequency shift does not go to zero even at Ar 0% condition in Figure 4.

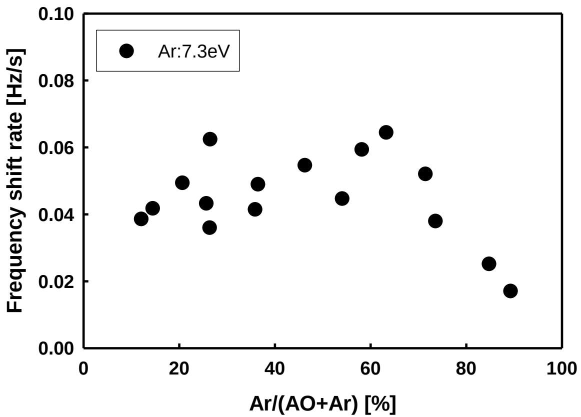

Figure 4 The frequency shift of PI-QCM during the exposure of various Ar fraction beam (7.3 eV)

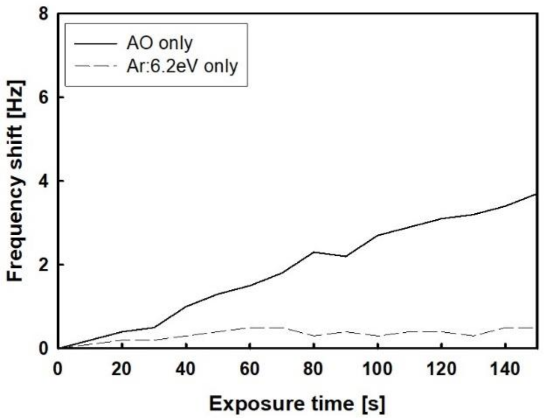

Figure 5 The frequency shift of the polyimide-coated QCM under exposure to AO beam and AO+Ar beam.

3.2 Mass-loss of PI-QCM under AO and Ar exposures

On the other hand, low Ar fraction conditions (<Ar 60%), the rate limiting step is considered to be CID process. If this hypothesis is correct, the rate of desorption (or rate of mass-loss) should be proportional to the Ar fraction and affected by collision energy in low Ar conditions where CID is the rate-limiting process. The same experiment was repeated with different collision energy of Ar at 5.8 and 4.2 eV. The results are shown in Figure 6 (a) and 6 (b) with the data of Ar 0% and Ar 100%. It is clearly identified that the frequency shift of PI-QCM increased, i.e., mass-decreased, with increasing Ar fraction in both cases as well as Figure 4. However, the expected collision energy dependence in frequency shift is not clearly observed in Figures 5 and 6.

The frequency shift of PI-QCM was normalized by Ar flux. The results are plotted in Figure 7. Data plots in three energies follow the same curve and the frequency shift of PI-QCM decreases rapidly in the Ar fraction between 10-60% and does not change much in the Ar fraction 60 to 90%. This analysis suggested that the effect of CID by Ar is similar in three collision energies tested and not effective in high Ar fraction condition over 60%. This is probably due to the fact that collision energy of 4-7 eV used in this experiment is too low to observe the clear energy dependence in CID process.

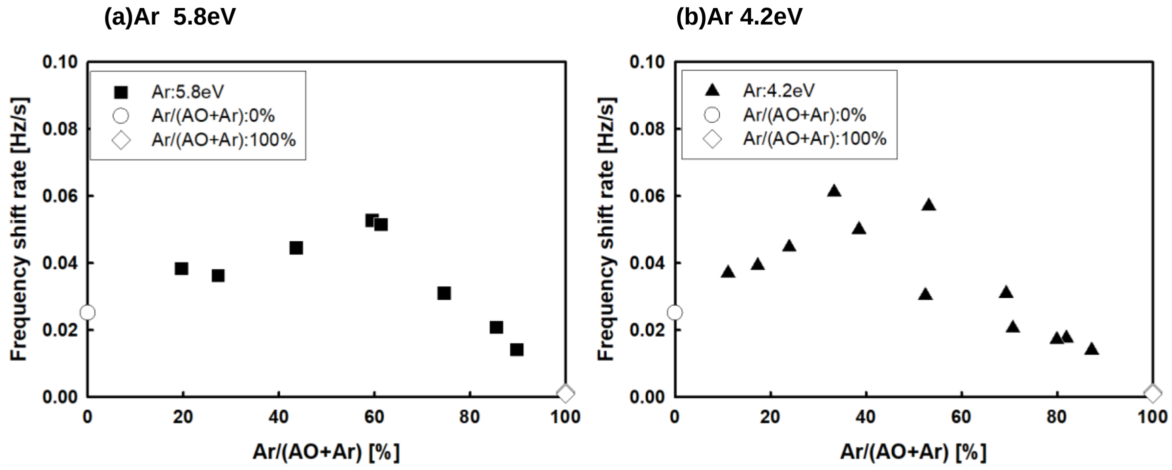

Figure 6 The frequency shift of PI-QCM during the exposure of various Ar fraction beam.

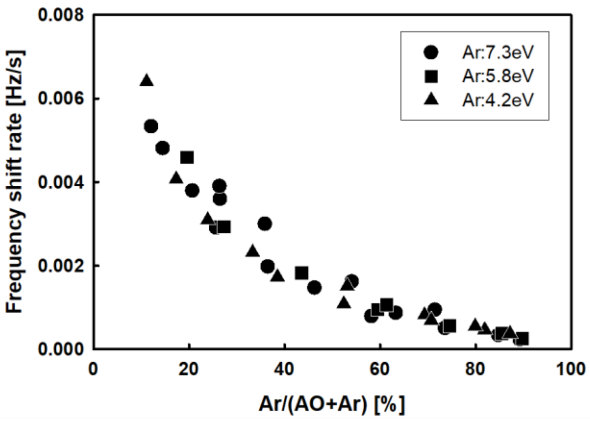

Figure 7 The frequency shift of PI-QCM was normalized by Ar flux.

3.3 Erosion yield (Ey) of PI in VLEO

The Ar fraction dependence on PI erosion shown in Figures 4 and 6 are converted to erosion yield (Ey) which is the eroded volume by collision of single AO in the unit of cm3/atom.

Resonance frequency of QCM is theoretically described in the formula below (Sauerbrey Equation) [7]:

$$\Delta f = -\frac{2Nf_0^2\Delta m}{A_E\sqrt{\mu\rho}}$$

Where
Δf: frequency shift *per second*, N: harmonic overtone, f_0: resonant frequency, Δm: mass, A_E: electrode area,
μ: shear modulus of quartz, and ρ: density of quartz, respectively. The figures listed below were used for the analysis: N$= 1$, f_0: $5.000\mathrm{E}+6$ Hz, $A_E = 1.038$ cm^2, $\mu = 2.947\mathrm{E}+11$ g/cm/s^2, and $\rho = 2.648$ g/cm^3. As a results, we obtain following relationship between Δf and Δm.

$$\frac{\Delta f}{\Delta m} = -5.455 \times 10^7\ [Hz/g]$$

Mass loss of PI is calculated from the frequency shift of PI-QCM by the equation below.

$$E_{yPI} = \frac{\Delta m}{\rho_{PI}F_{AO}A_{PI}}$$

Where, sample area $A_{PI} = 0.442$ cm^2, density of polyimide $\rho_{PI} = 1.43$ g/cm^3, and AO flux per second (Table 1) $F_{AO} = 3.22 \times 10^{14}$atoms/cm^2/s.

The eroded volume of PI is obtained by dividing by the density of PI. On the other hand, AO flux in all Ar conditions are calculated by AO flux per second shown in Table 1. Ey, thus calculated, is plotted against Ar fraction. The results are indicated in Figure 8. Ey at Ar 33% is 3.0E-24 which is the established value of Ey. It is clearly indicated that Ey increases linearly with Ar fraction due to CID effect by Ar. Ey at Ar 50% reaches 6.0E-24, twice as large as established value. CID effect by N_2 was measured by atomic oxygen fluence sensor (AOFS) mission aboard superlow altitude test satellite (SLATS). Detail of the AOFS mission analysis is describe elsewhere [8,9]. It was analyzed that Ey measured by AOFS-H7 sensor becomes 1.82 times greater than N_2 0% condition. The CID effect by Ar shown in this study qualitatively reproduces the CID effect of N_2 in VLEO measured by SLATS. From a series of ground-based experiments, it was concluded that the Ey of polyimide, which is used as a reference value of all material erosion experiment, depends on the N_2 fraction in the upper atmosphere of Earth.

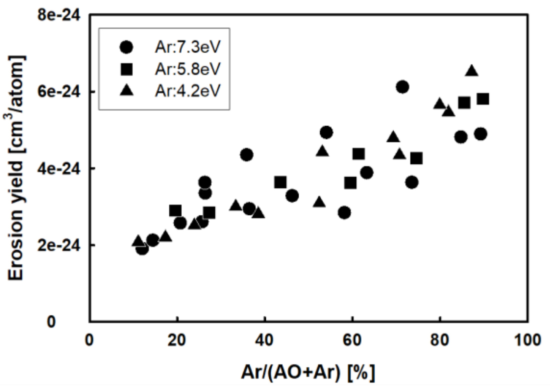

Figure 8 The erosion yield of PI. (Figures 4 and 6 are converted to erosion yield)

4. Conclusions

PI erosion in simultaneous collision of AO and Ar were studied by laser detonation facility with dual-PSV system in order to simulate material responses by AO and N_2 collisions in VLEO. It was clearly indicated that the degradation of PI is enhanced by CID effect by Ar. The experimental results were compared to the PI erosion data measured by SLATS in VLEO. Both results showed a good agreement. The findings obtained in this study gives a concrete evidence of the existence of CID effect by N_2 in VLEO. Because the material erosion in VLEO is accelerated by CID by N_2, this effect needs to take into consideration in a life-time assessment of materials used in VLEO environment.

Acknowledgments

This work was partially supported by the KAKENHI from JSPS under the contract numbers 18H01624, 18K148912, and 19H02346.

References

[1] T.K. Minton, J. Zhang, D. J. Garton and J. W. Seals, “Collision-assisted erosion of hydrocarbon polymers in atomic-oxygen environments,” High Performance Polymer, 12, 2000, pp.27-42

[2] Yokota, Kumiko, Tagawa, Masahito, Fujimoto, Yusuke, Ide, Wataru, Kimoto, Yugo, Tsuchiya, Yuta, Goto, Aki, Yukumatsu, Kazuki, Miyazaki, Eiji, Imamura, Shunsuke. (2021). Effect of simultaneous N2 collisions on atomic oxygen-induced polyimide erosion in sub-low Earth orbit: comparison of laboratory and SLATS data. CEAS Space Journal. 10.1007/s12567-021-00358-4.

[3] ASTM E2089-00, Standard Practices for Ground Laboratory Atomic Oxygen Interaction Evaluation of Materials for Space Applications, 2006

[4] Yokota, K., Yasuda, S., Mizutani, A., Tagawa, M.: Relative electron impaction probabilities of O, O2, and Ar components in laser-detonation hyperthermal beams, Japanese Journal of Applied Physics, Vol.52, 2013.

[5] Yokota, K., Kita, K., Okura, R., Shimizu, T., Chee, S.K., Iwata,M., Tagawa, M.: One-nozzle two-beam laser-detonation system.In: 14th International Symposium on Materials in the Space Environment/12th International Conference on protection of Materials and Structures in a Space Environment. Biarritz, France (2018)

[6] Kinoshita, H., Tagawa, M., Yokota, K., Ohnae, N. “Nonlinear phenomenon in the mass-loss of polyimide flm under hyperthermal atomic oxygen beam exposure.” High Perform. Polym. b13, 225–234 (2001)

[7] Sauerbrey, G.: Verwendung von schwingquarzen zur wägung dünner schichten und zur mikrowägung. Z. Phys. 159, 206–222 (1959)

[8] Imamura, S., Utashima, M., Ozawa, T., Akiyama, K., Sasaki, M.: Current status of the on-going orbit transfer of super low altitude test satellite (SLATS). In: Proceedings of the 69th International Astronautical Congress, IAC-18-C1.8.1. Bremen, Germany, 2018

[9] Tsuchiya, Y., Yukumatsu, K., Goto, A., Miyazaki, E., Kimoto, Y., Imamura, S., Miura, T., Sasaki, M., Operation results of atomic oxygen fluence sensor (AOFS) aboard SLATS satellite.